Opposing functions of the plant *TOPLESS* gene family during SNC1-mediated autoimmunity

Christopher M. Garner[a,b,c,1], Benjamin J. Spears[a,c], Jianbin Su[a,c], Leland Cseke[a,c], Samantha N. Smith[a,c], Conner J. Rogan[b,c,2], and Walter Gassmann[a,c,§]

[a]Division of Plant Sciences, University of Missouri, Columbia, MO 65211, USA

[b]Division of Biological Sciences, University of Missouri, Columbia, MO 65211, USA

[c]Christopher S. Bond Life Sciences Center and Interdisciplinary Plant Group, University of Missouri, Columbia, MO 65211, USA

[1]Current Address: Thermo Fisher Scientific, Carlsbad, CA

[2]Current Address: Oregon State University, Corvallis, OR

[§]Corresponding author: gassmannw@missouri.edu

Author contributions

Conceptualization: CMG, WG; formal analysis: CMG, BJS; funding acquisition: CMG, WG; investigation: CMG, BJS, JS, SNS, CJR; methodology: CMG, BJS, JS; project administration: CMG, WG; visualization: CMG, LC; writing - original: CMG; writing - review & editing: CMG, LC, WG

Short title: *TOPLESS-RELATED2* suppresses *SNC1*-mediated autoimmunity

Abstract

Regulation of the plant immune system is important for controlling the specificity and amplitude of responses to pathogens and in preventing growth-inhibiting autoimmunity that leads to reductions in plant fitness. In previous work, we reported that SRFR1, a negative regulator of effector-triggered immunity, interacts with SNC1 and EDS1. When *SRFR1* is non-functional in the Arabidopsis accession Col-0, *SNC1* levels increase, causing a cascade of events that lead to autoimmunity phenotypes. Previous work showed that some members of the transcriptional co-repressor family TOPLESS interact with SNC1 to repress negative regulators of immunity. Therefore, to explore potential connections between *SRFR1* and *TOPLESS* family members, we took a genetic approach that examined the effect of each *TOPLESS* member in the *srfr1* mutant background. The data indicated that an additive genetic interaction exists between *SRFR1* and two members of the *TOPLESS* family, *TPR2* and *TPR3*, as demonstrated by increased stunting and elevated *PR2* expression in *srfr1 tpr2* and *srfr1 tpr2 tpr3* mutants. Furthermore, the *tpr2* mutation intensifies autoimmunity in the auto-active *snc1-1* mutant, indicating a novel role of these *TOPLESS* family members in negatively regulating *SNC1*-dependent phenotypes. This negative regulation can also be reversed by overexpressing *TPR2* in the *srfr1 tpr2* background. Thus, this work uncovers diverse functions of individual members of the TOPLESS family in Arabidopsis and provides evidence for the additive effect of transcriptional and post-transcriptional regulation of *SNC1*.

41 **Author Summary**

42 The immune system is a double-edged sword that affords organisms with protection against infectious
43 diseases but can also lead to negative effects if not properly controlled. Plants only possess an innate
44 antimicrobial immune system that relies on rapid upregulation of defenses once immune receptors detect
45 the presence of microbes. Plant immune receptors known as resistance proteins play a key role in rapidly
46 triggering defenses if pathogens breach other defenses. A common model of unregulated immunity in
47 the reference Arabidopsis variety Columbia-0 involves a resistance gene called *SNC1*. When the SNC1
48 protein accumulates to unnaturally high levels or possesses auto-activating mutations, the visible
49 manifestations of immune overactivity include stunted growth and low biomass and seedset.
50 Consequently, expression of this gene and accumulation of the encoded protein are tightly regulated on
51 multiple levels. Despite careful study the mechanisms of *SNC1* gene regulation are not fully understood.
52 Here we present data on members of the well-known TOPLESS family of transcriptional repressors.
53 While previously characterized members were shown to function in indirect activation of defenses,
54 TPR2 and TPR3 are shown here to function in preventing high defense activity. This study therefore
55 contributes to the understanding of complex regulatory processes in plant immunity.

56

Introduction

Plants defend against infection by having a multilayered immune system, one branch of which recognizes molecular signatures of microbes through pattern recognition receptors at the cell surface. At the same time, plants monitor potential intracellular targets of pathogen attack [1,2]. At the heart of this intracellular plant surveillance system are the resistance genes of the nucleotide binding site – leucine-rich repeat (NLR) class [3]. Resistance proteins recognize, directly or indirectly, the actions of pathogen-secreted effector proteins which seek to interfere with plant immune responses or normal plant physiology. Upon sensing the activity of effectors, resistance proteins elicit a rapid and robust defense response, called effector-triggered immunity (ETI). In the case of the biotrophic defense response, this includes accelerated production of high levels of the plant hormone salicylic acid (SA) and the induction of *PATHOGENESIS RELATED* (*PR*) genes [1].

Because of cross-talk between plant hormone pathways, activation of the defense response is accompanied by repression of pathways that promote growth [4–7]. Therefore, induction of the plant immune system must be kept under tight control to avoid fitness penalties incurred during the absence of pathogen infection [8], as illustrated by autoimmune mutants of Arabidopsis that display the negative effects of an unregulated immune response. More than thirty different mutants have been identified that cause an autoimmune response exhibited by dwarfism, high levels of salicylic acid, constitutive defense gene expression, and subsequent increased resistance to pathogens [9]. Genetic analysis of these mutants has provided a wealth of information regarding the identity of positive and negative regulators of the immune response, and they illustrate the many levels of regulation that take place within the plant immune system.

SUPRESSOR of rps4-RLD1 (SRFR1) is a negative regulator of ETI mediated by several NLR proteins with a Toll/interleukin-1 receptor domain at their N-termini (TNLs), including RPS4/RRS1 and

SNC1 [10–12]. It was discovered in a genetic screen for mutants that were resistant to *Pseudomonas syringae pv. tomato* strain DC3000 expressing the bacterial effector AvrRps4 in the Arabidopsis accession RLD, which is normally susceptible because of natural inactivating polymorphisms in the *RPS4* resistance gene [10]. Mutants of *srfr1* in the Col-0 background constitutively activate SNC1 expression, causing an autoimmune phenotype characterized by high levels of salicylic acid, constitutive expression of PR genes, and severe stunting [12,13]. This autoimmune phenotype is absent in the RLD background due to an absence of a full-length *SNC1* allele [12]. SRFR1 interacts with the TNLs RPS4, RPS6, and SNC1 as well as the central ETI regulator EDS1 in a complex disrupted by AvrRps4 [2,14]. Furthermore, *srfr1 eds1* mutants lose increased resistance phenotypes [14]. These results place SRFR1 as a key regulator of effector-triggered immunity conferred by the TNL class of resistance genes.

In addition to interactions within an ETI protein complex, homology to transcriptional regulators and interaction with transcription factors suggest SRFR1 could also be part of a transcriptional repressor complex [11]. SRFR1 interacts with members of the TEOSINTE BRANCHED1-CYCLOIDEA-PROLIFERATING CELL FACTOR (TCP) transcription factor family in the nucleus. Specifically, SRFR1 interacts strongly with TCP8, TCP14, and TCP15, and a triple *tcp8 tcp14 tcp15* mutant is compromised in effector-triggered immunity [15]. This interaction between SRFR1 and positive ETI regulators suggests a model wherein SRFR1 is restricting TCP access to promoters of defense-related genes, or recruiting other proteins that function as repressors of transcription at these promoters.

The five member Arabidopsis *TOPLESS* gene family (*TPL*, *TOPLESS RELATED1, TPR2, TPR3,* and *TPR4*) encodes members of the larger GRO/TUP1 family of corepressors that are proposed to interact with DNA-binding proteins in the promoter regions of regulated genes to repress transcription [16]. Analysis of TPL/TPR family interactions with transcription factors indicates that they have been coopted multiple times to regulate gene expression in diverse processes, including control of flowering

time, hormone signaling, and stress responses [17]. Structural studies also provide evidence that TPL tetramerizes as part of its interactions with protein partners, suggesting the possibility of heterotetramers within the TOPLESS family [18].

Furthermore, TPR1 was shown to interact with SNC1, and together the complex, with an as yet unknown DNA-binding transcription factor, represses transcription of genes that function as negative regulators of defense responses such as *DEFENSE NO DEATH 1* (*DND1*) and *DND2*, which encode cyclic nucleotide-gated ion channels [19,20]. Therefore, similar to the interactions of SRFR1 with the TNL-mediated ETI machinery and transcription factors, TOPLESS family members display multiple mechanisms in their functions as co-repressors.

Whether SRFR1 is acting as part of a complex with the ETI machinery or functions as a transcriptional co-repressor, which molecular pathways regulate the autoimmunity phenotype of *srfr1* mutants remains a pressing question. Both models presented us with the possibility that *SRFR1* may also be interacting, at least genetically, with members of the TOPLESS family. Thus, we hypothesized that loss-of-function mutations in the *TOPLESS* gene family in the *srfr1-4* background would display similar phenotypes to the *tpl/tpr1* mutants in the *snc1-1* auto-active mutant background, reducing the *SNC1*-mediated autoimmune response. Here, we report the unexpected result that mutations in *TPR2* and *TPR3* have the opposite effect from those in *TPR1*, increasing the *SNC1* autoimmune response in the *srfr1-4* mutant background. This presents a novel function for TPR2 and TPR3 in either repressing positive regulators of the immune response or interfering with the SNC1-TPR1-mediated repression of negative regulators.

Results

Mutations in *TPR2* exacerbate the *srfr1-4* autoimmune phenotype

To investigate possible genetic interactions between *SRFR1* and members of the *TOPLESS* family, *srfr1-4* was crossed with T-DNA mutants in *TPL*, *TPR1*, *TPR2*, *TPR3*, and *TPR4*. Homozygous *srfr1-4 tpl/tpr* double mutants were compared to *srfr1-4* to determine if stunting, a measure of constitutively activated defenses, was affected. To quantify these differences in stunting we also measured shoot weights from each genotype after 4 weeks of growth. The results showed that *srfr1-4 tpl-8* and *srfr1-4 tpr2-2* were significantly different from *srfr1-4* in terms of size and overall shoot mass, in opposite directions (Fig 1). *PR2* is well established as an overall marker of immune system activation, and we found that the degree of stunting in this panel of auto-immune mutants correlated with their level of PR2 expression (S1 Fig). Stunting in *srfr1-4* is due to the activation of the TNL gene *SNC1* [13,19]. Given that it was shown that mutation of *tpl* lessens the effect of stunting in autoactive *snc1-1* mutants [19], and the dependency of stunting in *srfr1-4* on activation of *SNC1*, we concluded that the effect we were seeing in *srfr1-4 tpl-8* mutants was a recapitulation of previous findings and chose not to investigate this mutant any further. We did not see a similar phenotype in *srfr1-4 tpr1-2*, most likely because the *tpr1-2* allele used here is not a true knockout.

In contrast, the increased stunting of *srfr1-4 tpr2-2* represents a novel genetic interaction, and as such we switched our focus to concentrate on the *SRFR1-TPR2* interaction. To verify that the increased autoimmunity phenotype was indeed caused by the insertion at the *TPR2* locus and not some other tightly linked mutation, we obtained a second allele of *TPR2*, *tpr2-1*, and crossed this allele to *srfr1-4*. As with *srfr1-4 tpr2-2*, we saw increased stunting in the *srfr1-4 tpr2-1* double mutant relative to *srfr1-4* (Fig 2A). To quantify these differences in stunting we measured shoot weights from each genotype after 4 weeks of growth. The results showed that *srfr1-4 tpr2-1* and *srfr1-4 tpr2-2* were significantly different from *srfr1-*

148 *4* in terms of overall shoot mass (Fig 2B), but that neither *TPR2* single mutant was significantly different
149 from Col-0.
150
151 **_TPR2_ and _TPR3_ are partially redundant in repressing autoimmunity in _srfr1-4_**
152 Previous research has demonstrated functional redundancy amongst TOPLESS family members, and that
153 higher order *tpl/tpr* knockouts produce stronger phenotypes than single *tpl/tpr* mutants [21–23]. Based on
154 the close evolutionary relatedness of *TPR2* and *TPR3* (S2 Fig) and previous reports that indicated *TPL*,
155 *TPR1*, and *TPR4* are repressors of negative regulators of immunity [19], we chose to investigate if
156 mutations in *TPR3* would impact the *srfr1-4 tpr2-2* phenotype. To obtain a *srfr1-4 tpr2-2 tpr3-1* triple
157 mutant, *srfr1-4 tpr2-2* was crossed with *srfr1-4 tpr3-1*. Analysis of shoot mass showed that the *srfr1-4*
158 *tpr2-2 tpr3-1* triple mutant is significantly smaller than both *srf1-4* and *srfr1-4 tpr2-2* (Fig3A and Fig3B).
159 As TOPLESS family members have been shown to be repressors of transcription we decided to
160 examine the mRNA levels of *SNC1* in the *srfr1-4 tpr2-2* and *srfr1-4 tpr2-2 tpr3-1* mutants to see if they
161 were affected relative to *srfr1-4*. We also examined *PR2* expression as a marker for overall immune
162 activation and used qPCR rather than protein blotting to quantify subtle differences in mRNA levels for
163 the remainder of this study. As illustrated in Fig 3C and 3D, *PR2* and *SNC1* mRNA levels were
164 significantly increased in *srfr1-4 tpr2-2* and *srfr1-4 tpr2-2 tpr3-1* relative to *srfr1-4*; however, no
165 significant change in *PR2* or *SNC1* expression was observed in the *tpr2-2* or *tpr3-1* single mutants.
166 Given the partial redundancy observed between *TPR2* and *TPR3* in the *srfr1-4* background and the
167 lack of any observable phenotype in the single mutants, we crossed *tpr2-2* to *tpr3-1* to create a *tpr2-2*
168 *tpr3-1* double mutant. No stunting or other morphological phenotypes were observed in *tpr2-2 tpr3-1* (Fig
169 4A). We also found no significant difference between Col-0 and *tpr2-2 tpr3-1* with regards to *PR2*

expression; however, we did see a small but significant increase in *SNC1* expression in *tpr2-2 tpr3-1* when compared to Col-0 (Fig 4C and 4D).

Overexpression of *TPR2* in the *srfr1-4* background represses autoimmunity

We next asked if overexpressing *TPR2* would have the opposite effect and suppress autoimmunity in the *srfr1-4 tpr2-2* background. To test this hypothesis we cloned the *TPR2* coding sequence as a translational fusion with a C-terminal 10xMyc tag behind the constitutively active cauliflower mosaic virus 35S promoter. Using the 35S:*TPR2-myc* construct, several stable lines were created in the *srfr1-4 tpr2-2* genetic background. Two independent homozygous *TPR2-myc srfr1-4 tpr2-2* lines in the T3 generation, were planted alongside Col-0, *srfr1-4*, and *srfr1-4 tpr2-2* to compare the degree of stunting. At four weeks after planting, the *TPR2-myc srfr1-4 tpr2-2* plants were less stunted than both *srfr1-4 tpr2-2* and *srfr1-4* (Fig 5A).

Quantification of *SNC1* showed that not only was transcript level reduced below *srfr1-4 tpr2-2* levels, but was also less than *SNC1* levels in *srfr1-4* (Fig 5B), correlating with plant size (Fig 5A). The TNL gene *RPP4* is located within the *SNC1* locus and has been shown to be co-regulated with *SNC1* both at the level of transcription and after transcription by RNA silencing [24]. We have also previously shown that *RPP4* is upregulated in *srfr1-4* [12]. To determine if *TPR2* also affects *RPP4* expression in the *srfr1-4* background, we quantified *RPP4* mRNA in *srfr1-4 tpr2-2* and in *TPR2-myc srfr1-4 tpr2-2*. We saw a slight non-significant increase in *RPP4* expression in *srfr1-4 tpr2-2* relative to *srfr1-4*, while *RPP4* mRNA was reduced in *TPR2-myc srfr1-4 tpr2-2* below levels in *srfr1-4* (Fig 5C).

Increased autoimmunity in *srfr1-4 tpr2-2* is partially dependent upon *SNC1*

Previous work has shown that stunting in *srfr1-4* is dependent on *SNC1*, and that a *srfr1-4 snc1-11* double mutant is morphologically normal but still expresses higher than normal levels of several defense-related genes [12]. To see if the enhanced autoimmunity that results from mutating *TPR2* in the *srfr1-4* background is dependent on *SNC1*, we created a quadruple mutant by crossing the *SNC1* knockout allele, *snc1-11*, to *srfr1-4 tpr2-2 tpr3-1*. As was previously observed for *srfr1-4 snc1-11*, we saw no stunting or morphological abnormalities in the *srfr1-4 snc1-11 tpr2-2 tpr3-1* quadruple mutant (Fig 6A). *SRFR1* regulation of *RPP4* is *SNC1* independent as *RPP4* is upregulated equally in both *srfr1-4* and *srfr1-4 snc1-11* relative to wild type levels in Col-0 [12]. Interestingly, *RPP4* expression was significantly decreased both in *srfr1-4 snc1-11 tpr2-2 tpr3-1* compared to *srfr1-4 snc1-11* and in *snc1-11 tpr2-2 tpr3-1* compared to *snc1-11* (Fig 6B), whereas *RPP4* mRNA levels in the *srfr1-4 tpr2-2* mutant were slightly higher than in *srfr1-4* (Fig 5C), indicating that these higher *RPP4* mRNA levels are at least partially dependent upon *SNC1*. Consistent with our previous study, we saw an increase in *PR2* levels in the *srfr1-4 snc1-11* double mutant compared to Col-0 and *snc1-11*. *PR2* levels in *srfr1-4 snc1-11 tpr2-2 tpr3-1* were comparable to those in *srfr1-4 snc1-11* (Fig 5C).

To further investigate the relationship between *TPR2* and *SNC1* activity, we crossed *tpr2-2* to *snc1-1*, an auto-active allele of *SNC1* that induces a constitutive defense response and associated stunting [25]. The F2 from this cross produced approximately 1/16th plants which genotyped as homozygous *snc1-1 tpr2-2* that were extremely stunted and produced very little seed. When compared to *snc1-1*, *snc1-1 tpr2-2* was significantly more stunted, and had significantly higher levels of *SNC1* and *PR2* mRNA (Fig 7). These results are consistent with the conclusion that the autoimmune phenotypes modulated by mutations in *SRFR1* and *TPR2* are tightly associated with *SNC1*.

SRFR1 acts upstream of _SNC1_ transcription

Transcription of *SNC1* is subject to feedback regulation through the production of salicylic acid. Upon activation of SNC1, SA accumulates in the plant and increased levels of SA cause even more transcription of *SNC1* [26]. Our data show that *tpr2-2* increases *SNC1* mRNA levels in the *srfr1-4* and *snc1-1* backgrounds, but because of the complex feedback regulation of *SNC1* transcription it is unclear whether *SRFR1* and *TPR2* are directly affecting transcription at the *SNC1* locus, or if they are repressing some component downstream of SNC1 activation. Signaling for all Arabidopsis TNL class resistance proteins identified to date is dependent upon EDS1 [27], and mutating *EDS1* blocks the feedback regulation of SNC1, thereby making it possible to disambiguate events upstream of *SNC1* transcription from events downstream of SNC1 activation [28]. The *eds1-2* allele is a knockout for *EDS1* introgressed into Col-0 [29]. Previous work has shown that a *srfr1-4 eds1-2* double mutant shows no signs of enhanced basal resistance and is morphologically indistinguishable from Col-0 [14].

To determine if the *tpr2-2* mutation had any effect on transcription of *SNC1* in *srfr1-4 eds1-2*, we crossed *eds1-2* to *tpr2-2* and *srfr1-4 tpr2-2* to *srfr1-4 eds1-2* and obtained *eds1-2 tpr2-2* and *srfr1-4 eds1-2 tpr2-2* mutants. As seen previously with the *srfr1-4 eds1-2* double mutant, the *srfr1-4 eds1-2 tpr2-2* triple mutant was not morphologically different from Col-0 (Fig 8A). When we quantified the amount of *SNC1* transcript in these plants we found that *srfr1-4 eds1-2* produced significantly more *SNC1* than Col-0, *eds1-2*, and *eds1-2 tpr2-2* (Fig 8B). The *srfr1-4 eds1-2 tpr2-2* triple mutant had a repeatable but non-significant increase in *SNC1* relative to *srfr1-4 eds1-2* (Fig 8B). These data suggest that *SRFR1* also acts upstream of *SNC1* transcription, while *TPR2* acts downstream of *SNC1* transcription.

TPR1 was previously shown to directly interact with the TIR domain of SNC1 [19]. To determine if TPR2 interacts with SNC1, we performed an *in vitro* pull down assay between GST-tagged TPR2 and T7-tagged SNC1-TIR domain. Pull down of GST-TPR2 with GST beads co-precipitated T7-

238 SNC1-TIR, whereas pull down of GST alone failed to co-precipitate T7-SNC1-TIR (Fig 8C), indicative
239 of a direct protein-protein interaction between TPR2 and SNC1. The post-transcriptional activity of
240 TPR2 may therefore consist of competing with TPR1 for binding of SNC1.
241
242 **Discussion**
243
244 To determine whether members of the *TPL* transcriptional repressor gene family functionally interact
245 with *SRFR1* we chose a genetic approach. By creating double and higher order mutants between *srfr1-4*,
246 members of the *TOPLESS* family, and other genes relevant to the *srfr1-4* autoimmune phenotype, we
247 were able to assess the impact these genes had on constitutive immunity. Our results indicate a genetic
248 interaction between *SRFR1* and *TPR2* and its close homolog *TPR3*. Further data show a novel genetic
249 interaction between *SNC1* and *TPR2*. We found that stunting in *srfr1-4* was affected by mutations in
250 *TPL* and *TPR2*, but in opposite ways; *srfr1-4 tpl-8* was less stunted, and *srfr1-4 tpr2-2* was more
251 stunted. To verify that these phenotypes were a consequence of altered immune system regulation, and
252 not a developmental phenotype unrelated to defense, we measured the expression of *PR2* as a marker of
253 the defense response [30,31]. Previous research has shown that *PR1* and *PR2* mRNA levels are elevated
254 in *srfr1-4* relative to wild type plants [12]. Here, we found that *PR2* levels in *srfr1-4 tpl-8* and *srfr1-4*
255 *tpr2-2* are indeed consistent with differentially regulated immune system outputs in these double
256 mutants.
257
258 **Contrasting roles of *TPR1/TPL* and *TPR2/TPR3***
259 Stunting, but not all aspects of heightened basal resistance in *srfr1-4* has been previously shown to be
260 dependent upon the TNL gene *SNC1* [12]. One mechanism by which SNC1 activates the immune

261 system was demonstrated to be through a protein interaction with TPR1, the end result of this interaction
262 being the repression of negative regulators of defense such as *DND1* and *DND2*. *SNC1* was also shown
263 to interact genetically with *TPL*, which shares 92% identity with TPR1 at the amino acid level [19]. The
264 attenuated autoimmunity we observed in *srfr1-4 tpl-8* is in agreement with this model. We did not see a
265 similar phenotype in *srfr1-4 tpr1-2*, most likely because the *tpr1-2* allele is not a true knockout. We
266 verified by sequencing out from the T-DNA that the location of the *tpr1-2* insertion is within the first
267 intron of *TPR1*, which is located in the 5' untranslated region. This insertion may not be sufficient to
268 knock out transcription of functional *TPR1* mRNA.

269 In contrast to *srfr1-4 tpl-8*, the *srfr1-4 tpr2-2* phenotype is a novel case wherein a member of the
270 *TOPLESS* family is implicated in repressing an immune response. Based on the strikingly different
271 phenotypes of the double mutants we propose that TPR2 is repressing a set of genes disparate from that
272 of TPR1 or is activating genes in the *srfr1-4* background. We verified that the exacerbated autoimmune
273 phenotype in *srfr1-4 tpr2-2* was linked to *TPR2* by demonstrating that another allele of *TPR2*, *tpr2-1*,
274 could produce the same phenotype in *srfr1-4*.

275 Previous research has shown varying degrees of redundancy amongst the different members of
276 the *TOPLESS* family depending on the process under study. In embryogenesis and circadian clock
277 regulation, knocking out all *TPL/TPR* genes is required to see a phenotype [21,32], whereas the
278 repression of brassinosteroid-sensitive genes via BZR1 requires specifically TPL, TPR1, and TPR4 [23].
279 Here we show that *TPR3*, the closest homolog of *TPR2*, has some functional redundancy with *TPR2* in
280 repressing autoimmunity in *srfr1-4* in that the *srfr1-4 tpr2-2 tpr3-1* triple mutant is significantly more
281 stunted than *srfr1-4 tpr2-2* and shows increased *PR2* levels relative to *srfr1-4 tpr2-2* and *srfr1-4*.
282

283 **Contributions to *SNC1* regulation by *SRFR1***

Although stunting in *srfr1-4* is fully dependent upon *SNC1*, *SRFR1* has a broader effect on immune function independent of *SNC1*. The TNL resistance genes *RPS4*, *RPP4*, and At4g16950 are all upregulated in *srfr1* mutants independent of *SNC1*, as well as several other genes related to immune function such as *EDS1*, *PAD4*, *SID2*, *PR1*, and *PR2* [11,12]. *SNC1* is located within the *RPP5* disease resistance locus, a complex locus containing several paralogous resistance genes [33]. It has been previously shown that activation of SNC1 leads to increased transcription of other resistance genes at this locus, such as *RPP4* and *At4g16950* [12,24,34]. The mechanism by which *RPP4* and *At4g16950* are upregulated by activated SNC1 is unknown, although two possibilities were proposed in Yi and Richards. The first involves upregulation as a result of increased SA caused by SNC1 activation, citing previous work showing that application of SA is sufficient to cause a large increase in *SNC1* transcript [26]. However, they also do not rule out the possibility that chromatin structure at the locus might be altered due to increased transcription of *SNC1,* creating a permissive environment for transcription of neighboring paralogs [24].

Interestingly, *RPP4* and *At4g16950* are both upregulated in *srfr1-4 snc1-11* [12], a genetic background without a functional copy of *SNC1*, and as a consequence of this observation we hypothesized that the *PR2* increase we observed in *srfr1-4 snc1-11 tpr2-2 tpr3-1* could be due to a further increase in transcript of these other *RPP5* locus resistance genes. Surprisingly, *RPP4* levels were significantly decreased by adding the *tpr2* and *tpr3* mutations to *srfr1-4 snc1-11*, implying that the increased *RPP4* in *srfr1-4 tpr2-2* relative to *srfr1-4* is fully dependent upon increased *SNC1*. We therefore asked if *TPR2* had a genetic interaction with *SNC1* by crossing *tpr2-2* with *snc1-1*. The *snc1-1* allele contains a point mutation in the linker region between the NBS and LRR domains that causes constitutive activation of the SNC1 protein and associated stunting caused by induction of the defense response without increasing the levels of *snc1-1* mRNA [25,35]. In the *snc1-1 tpr2-2* double mutant we

307 saw significantly increased stunting, and *snc1-1* and *PR2* mRNA levels, suggesting a role for *TPR2* in
308 the downregulation of the SNC1-mediated constitutive defense response.

309 In order for resistance genes of the TNL class to function, the lipase like protein EDS1 must be
310 present [36–38]. To elucidate the position of *TPR2* in the *SNC1*-mediated constitutive defense response
311 we took advantage of the *srfr1-4 eds1-2* double mutant which blocks increased basal resistance in *srfr1-*
312 *4* [14] and consequently feedback upregulation of *SNC1*. Other studies have used mutations in *EDS1*,
313 and closely related protein interactor *PAD4* which is also required for *SNC1* signaling, to block feedback
314 upregulation of *SNC1* to determine if genes are acting upstream or downstream of SNC1 activation
315 [25,26,28,39]. In the *srfr1-4 eds1-2 tpr2-2* triple mutant we did not see a significant increase in *SNC1*
316 mRNA absent of SNC1 protein activation compared to *srfr1-4 eds1-2*. This result implies that *TPR2* is
317 acting downstream of SNC1 activation, whereas *SRFR1* also impacts the level of *SNC1* mRNA. This
318 difference may be one component for the additive effect of mutations in *SRFR1* and *TPR2* on the level
319 of constitutively activated defenses.

320

321 **Model for TPR2/TPR3 and SRFR1 functions in SNC1-mediated autoimmunity**

322 Based on these data we present the following model for TPR2 and SRFR1 function in autoimmunity
323 caused by SNC1 activation (Fig 9). In the *srfr1-4* background *SNC1* mRNA is expressed at a high level
324 and SNC1 is constitutively activated [12]. Disruption of protein-protein interactions between SRFR1 and
325 SNC1 [12] could lead to SNC1 activation; however, increased mRNA levels can also lead to SNC1 auto-
326 activation [24,40] and based on SRFR1's interaction with TCP transcription factors a direct regulation of
327 *SNC1* transcript levels [15,41] is consistent with the data obtained in the *eds1-2* background. Because in
328 wild type plants levels of *SNC1* are kept low to avoid fitness penalties, the effects of *TPR2* mutations are
329 only apparent when *SNC1* transcription is induced, such as in the autoimmune mutants *srfr1-4* and *snc1-*

1. We hypothesize that TPR2, and to some degree TPR3, acts downstream of *SNC1* transcription by repressing expression of a positive regulator of *SNC1* or activating a negative regulator. The physical interaction of TPR2 with the TIR domain of SNC1 shown here raises the possibility that TPR2 competes with TPR1 for binding of SNC1, and that TPR1-SNC1 and TPR2-SNC1 complexes regulate target genes such as *DND1* and *DND2* in opposite ways. In addition, enhancement of the *snc1-1* phenotype by *tpr2-2* illustrates that the enhanced resistance phenotype is not dependent upon mutations in *SRFR1*. Together, this suggests that TPR2 and SRFR1 are involved in separate pathways converging on regulation of SNC1.

Materials and Methods

Plant lines

Plant lines used for genetic analysis were *tpl-8* (SALK_036566), *tpr1-2* (SALK_065650C), *tpr2-1* (SALK_112730), *tpr2-2* (SALK_079848C), *tpr3-1* (SALK_029936), *tpr4-1* (SALK_150008), *snc1-11* (SALK_047058) from the Salk T-DNA knockout collection [42]. The *srfr1-4* line (SAIL_412-E08) was from the Syngenta Arabidopsis Insertion Library [43]. Salk and SAIL lines were acquired from the Arabidopsis Biological Resource Center. The *eds1-2* line was a gift from Jane Parker, and the *snc1-1* line was a gift from Harrold van den Burg. All mutants are in the Col-0 background, and genotyping primers used for these lines are detailed in Table S1. After parental lines were crossed, plants were genotyped in the F1 generation to verify the success of the cross, and then in the F2 generation to identify plants homozygous for the desired mutations.

Molecular cloning and generation of transgenic lines

352 The TPR2-myc construct was created by amplifying the *TPR2* CDS with flanking SpeI and PacI sites at
353 the 5' and 3' ends, respectively. The binary vector pGWB20 [44] was cut with XbaI and PacI to excise
354 the Gateway cassette, and the SpeI-*TPR2*-PacI fragment was ligated into the XbaI and PacI sites in frame
355 with the C-terminal myc tags in pGWB20. Sequencing was used to verify the clone. *Agrobacterium*
356 *tumefaciens* strain C58-C1 was transformed with the TPR2-myc construct by electroporation. The *srfr1-*
357 *4 tpr2-2* double mutant was grown at high temperatures to relieve stunting, and these plants were
358 transformed by floral dip. Transgenic seed was selected on hygromycin B, and T3 homozygotes were
359 selected by true breeding on selection plates. TPR2-myc protein expression was verified by western blot
360 using c-Myc antibody sc-789 (Santa Cruz Biotechnology, Dallas, TX, USA).

361 The GST-TPR2 construct was created by amplifying the *TPR2* CDS with flanking EcoRI and NotI
362 sites with an additional base between the EcoRI site and the start codon. The EcoRI-*TPR2*-NotI fragment
363 was cloned into pGEX-4T-3 (SigmaAldrich, St. Louis, MO, USA) digested with EcoRI and NotI.
364 Similarly, a cDNA encoding the SNC1 TIR domain (amino acids 1-182) was amplified with flanking
365 EcoRI and XhoI sites. The EcoRI-*TIR*-XhoI fragment was cloned into pET28a (EMD Millipore, Billerica,
366 MA USA) digested with EcoRI and XhoI to create *His-T7-SNC1 TIR*.

367

368 **RNA extraction, cDNA preparation and qPCR**

369 For qPCR experiments multiple plants from each genotype were ground together in liquid nitrogen to
370 form one replicate. For each experiment two or three replicates were used per genotype. After grinding
371 plant tissue in liquid nitrogen, total RNA was extracted using TRIZOL reagent (Thermo Fisher Scientific,
372 Carlsbad, CA, USA). First strand cDNA synthesis was carried out using 2 ug of total RNA and reverse
373 transcription was performed using an oligo (dT) 15 primer and Moloney murine leukemia virus (MMLV)
374 reverse transcriptase (Promega, Madison, WI, USA). qPCR was carried out using SYBR GREEN PCR

Master Mix (Thermo Fisher Scientific) or Brilliant III Ultra-Fast SYBR Green qPCR Master Mix (Agilent, Santa Clara, CA, USA) on either an ABI 7500 or Agilent AriaMX qPCR system. Transcript levels were normalized using *SAND* gene (At2g28390) for qPCR experiments. LinRegPCR was used to determine PCR efficiency and cycle thresholds for each sample [45], and the $2^{-\Delta\Delta C_T}$ method was used to determine expression levels [46]. Primers used for qPCR are detailed in Table S2.

Protein pull-down assays

GST-TPR2, empty pGEX-4T-3, and T7-SNC1-TIR in *E. coli* strain BL21(DE3) were streaked to single colonies and then incubated overnight at 37°C in LB broth. 200 ml of LB was inoculated with 2 ml of overnight culture and incubated for approximately 3 hours to an optical density of 0.6-0.8. IPTG at 500 µM was added to each culture and flasks were grown overnight at 22°C. Each culture was passed through a French press to lyse the cells. Extracts were centrifuged and 25 µl of GST beads (G-Biosciences, St. Louis, MO USA) were added to 6 µl supernatant of GST-TPR2 and empty pGEX-4T-3. Samples were incubated at 4°C for 1.5 hours with rotation. After washing 3 times with PBS, 6 µl soluble protein T7-SNC1-TIR was added, and samples were incubated at 4°C for 1 hour. After washing 3 times with PBS protein was eluted from beads in Laemmli buffer and then used for protein blot with anti-GST and anti-T7 (EMD Millipore). For PR2 detection in S1 Fig, PR2 antibody AS207 208 (Agrisera, Vannas, Sweden) was used.

Acknowledgements

We thank Harrold van den Burg for the *snc1-1* plant line, Gary Stacey for the pGWB20 vector, and Daniel Leuchtman and Sanzida Rahman for help with statistical analyses.

References

1. Cui H, Tsuda K, Parker JE. Effector-Triggered Immunity: From Pathogen Perception to Robust Defense. Annu Rev Plant Biol. 2015;66: 487–511. doi:10.1146/annurev-arplant-050213-040012
2. Su J, Spears BJ, Kim SH, Gassmann W. Constant vigilance: plant functions guarded by resistance proteins. Plant J Cell Mol Biol. 2018;93: 637–650. doi:10.1111/tpj.13798
3. Li X, Kapos P, Zhang Y. NLRs in plants. Curr Opin Immunol. 2015;32: 114–121. doi:10.1016/j.coi.2015.01.014
4. Huot B, Yao J, Montgomery BL, He SY. Growth-defense tradeoffs in plants: a balancing act to optimize fitness. Mol Plant. 2014;7: 1267–1287. doi:10.1093/mp/ssu049
5. Lozano-Durán R, Zipfel C. Trade-off between growth and immunity: role of brassinosteroids. Trends Plant Sci. 2015;20: 12–19. doi:10.1016/j.tplants.2014.09.003
6. Karasov TL, Chae E, Herman JJ, Bergelson J. Mechanisms to Mitigate the Trade-Off between Growth and Defense. Plant Cell. 2017;29: 666–680. doi:10.1105/tpc.16.00931
7. Guo Q, Yoshida Y, Major IT, Wang K, Sugimoto K, Kapali G, et al. JAZ repressors of metabolic defense promote growth and reproductive fitness in Arabidopsis. Proc Natl Acad Sci U S A. 2018;115: E10768–E10777. doi:10.1073/pnas.1811828115
8. van Butselaar T, Van den Ackerveken G. Salicylic Acid Steers the Growth-Immunity Tradeoff. Trends Plant Sci. 2020;25: 566–576. doi:10.1016/j.tplants.2020.02.002
9. van Wersch R, Li X, Zhang Y. Mighty Dwarfs: Arabidopsis Autoimmune Mutants and Their Usages in Genetic Dissection of Plant Immunity. Front Plant Sci. 2016;7: 1717. doi:10.3389/fpls.2016.01717

10. Kwon SI, Koczan JM, Gassmann W. Two Arabidopsis srfr (suppressor of rps4-RLD) mutants exhibit avrRps4-specific disease resistance independent of RPS4. Plant J Cell Mol Biol. 2004;40: 366–375. doi:10.1111/j.1365-313X.2004.02213.x

11. Kim SH, Kwon SI, Bhattacharjee S, Gassmann W. Regulation of defense gene expression by Arabidopsis *SRFR1*. Plant Signal Behav. 2009;4: 149–150. doi:10.4161/psb.4.2.7682

12. Kim SH, Gao F, Bhattacharjee S, Adiasor JA, Nam JC, Gassmann W. The Arabidopsis resistance-like gene *SNC1* is activated by mutations in *SRFR1* and contributes to resistance to the bacterial effector AvrRps4. PLoS Pathog. 2010;6: e1001172. doi:10.1371/journal.ppat.1001172

13. Li Y, Li S, Bi D, Cheng Y-T, Li X, Zhang Y. (2010) SRFR1 negatively regulates plant NB-LRR resistance protein accumulation to prevent autoimmunity. PLoS Pathog 6: e1001111. doi:10.1371/journal.ppat.1001111

14. Bhattacharjee S, Halane MK, Kim SH, Gassmann W. Pathogen effectors target Arabidopsis EDS1 and alter its interactions with immune regulators. Science. 2011;334: 1405–1408. doi:10.1126/science.1211592

15. Kim SH, Son GH, Bhattacharjee S, Kim HJ, Nam JC, Nguyen PDT, et al. The Arabidopsis immune adaptor SRFR1 interacts with TCP transcription factors that redundantly contribute to effector-triggered immunity. Plant J Cell Mol Biol. 2014;78: 978–989. doi:10.1111/tpj.12527

16. Lee JE, Golz JF. Diverse roles of Groucho/Tup1 co-repressors in plant growth and development. Plant Signal Behav. 2012;7: 86–92. doi:10.4161/psb.7.1.18377

17. Causier B, Ashworth M, Guo W, Davies B. The TOPLESS interactome: a framework for gene repression in Arabidopsis. Plant Physiol. 2012;158: 423–438. doi:10.1104/pp.111.186999

18. Martin-Arevalillo R, Nanao MH, Larrieu A, Vinos-Poyo T, Mast D, Galvan-Ampudia C, et al. Structure of the Arabidopsis TOPLESS corepressor provides insight into the evolution of transcriptional repression. Proc Natl Acad Sci U S A. 2017;114: 8107–8112. doi:10.1073/pnas.1703054114

19. Zhu Z, Xu F, Zhang Y, Cheng YT, Wiermer M, Li X, et al. Arabidopsis resistance protein SNC1 activates immune responses through association with a transcriptional corepressor. Proc Natl Acad Sci U S A. 2010;107: 13960–13965. doi:10.1073/pnas.1002828107

20. Niu D, Lin X-L, Kong X, Qu G-P, Cai B, Lee J, et al. SIZ1-Mediated SUMOylation of TPR1 Suppresses Plant Immunity in Arabidopsis. Mol Plant. 2019;12: 215–228. doi:10.1016/j.molp.2018.12.002

21. Long JA, Ohno C, Smith ZR, Meyerowitz EM. TOPLESS regulates apical embryonic fate in Arabidopsis. Science. 2006;312: 1520–1523. doi:10.1126/science.1123841

22. Wang Y, An C, Zhang X, Yao J, Zhang Y, Sun Y, et al. The Arabidopsis elongator complex subunit2 epigenetically regulates plant immune responses. Plant Cell. 2013;25: 762–776. doi:10.1105/tpc.113.109116

23. Oh E, Zhu J-Y, Ryu H, Hwang I, Wang Z-Y. TOPLESS mediates brassinosteroid-induced transcriptional repression through interaction with BZR1. Nat Commun. 2014;5: 4140. doi:10.1038/ncomms5140

461 **24.** Yi H, Richards EJ. A Cluster of Disease Resistance Genes in Arabidopsis Is Coordinately
462 Regulated by Transcriptional Activation and RNA Silencing. Plant Cell. 2007;19: 2929–
463 2939. doi:10.1105/tpc.107.051821
464 **25.** Zhang Y, Goritschnig S, Dong X, Li X. A Gain-of-Function Mutation in a Plant Disease
465 Resistance Gene Leads to Constitutive Activation of Downstream Signal Transduction
466 Pathways in *suppressor of npr1-1, constitutive 1*. Plant Cell. 2003;15: 2636–2646.
467 doi:10.1105/tpc.015842
468 **26.** Yang S, Hua J. A Haplotype-Specific Resistance Gene Regulated by *BONZAI1* Mediates
469 Temperature-Dependent Growth Control in Arabidopsis. Plant Cell. 2004;16: 1060–1071.
470 doi:10.1105/tpc.020479
471 **27.** Kim T-H, Kunz H-H, Bhattacharjee S, Hauser F, Park J, Engineer C, et al. Natural variation
472 in small molecule-induced TIR-NB-LRR signaling induces root growth arrest via EDS1-
473 and PAD4-complexed R protein VICTR in Arabidopsis. Plant Cell. 2012;24: 5177–5192.
474 doi:10.1105/tpc.112.107235
475 **28.** Huang S, Chen X, Zhong X, Li M, Ao K, Huang J, et al. Plant TRAF Proteins Regulate
476 NLR Immune Receptor Turnover. Cell Host Microbe. 2016;20: 271.
477 doi:10.1016/j.chom.2016.07.005
478 **29.** Bartsch M, Gobbato E, Bednarek P, Debey S, Schultze JL, Bautor J, et al. Salicylic Acid–
479 Independent ENHANCED DISEASE SUSCEPTIBILITY1 Signaling in Arabidopsis
480 Immunity and Cell Death Is Regulated by the Monooxygenase *FMO1* and the Nudix
481 Hydrolase *NUDT7*. Plant Cell. 2006;18: 1038–1051. doi:10.1105/tpc.105.039982

482 **30.** Dong X, Mindrinos M, Davis KR, Ausubel FM. Induction of Arabidopsis defense genes by
483 virulent and avirulent Pseudomonas syringae strains and by a cloned avirulence gene. Plant
484 Cell. 1991;3: 61–72. doi:10.1105/tpc.3.1.61
485 **31.** Cordelier S, de Ruffray P, Fritig B, Kauffmann S. Biological and molecular comparison
486 between localized and systemic acquired resistance induced in tobacco by a Phytophthora
487 megasperma glycoprotein elicitin. Plant Mol Biol. 2003;51: 109–118.
488 doi:10.1023/a:1020722102871
489 **32.** Wang L, Kim J, Somers DE. Transcriptional corepressor TOPLESS complexes with
490 pseudoresponse regulator proteins and histone deacetylases to regulate circadian
491 transcription. Proc Natl Acad Sci. 2013;110: 761–766. doi:10.1073/pnas.1215010110
492 **33.** Noël L, Moores TL, van Der Biezen EA, Parniske M, Daniels MJ, Parker JE, et al.
493 Pronounced intraspecific haplotype divergence at the RPP5 complex disease resistance
494 locus of Arabidopsis. Plant Cell. 1999;11: 2099–2112.
495 **34.** Zou B, Yang D-L, Shi Z, Dong H, Hua J. Monoubiquitination of histone 2B at the disease
496 resistance gene locus regulates its expression and impacts immune responses in
497 Arabidopsis. Plant Physiol. 2014;165: 309–318. doi:10.1104/pp.113.227801
498 **35.** Li X, Clarke JD, Zhang Y, Dong X. Activation of an EDS1-mediated *R*-gene pathway in
499 the *snc1* mutant leads to constitutive, NPR1-independent pathogen resistance. Mol Plant-
500 Microbe Interact MPMI. 2001;14: 1131–1139. doi:10.1094/MPMI.2001.14.10.1131
501 **36.** Parker JE, Holub EB, Frost LN, Falk A, Gunn ND, Daniels MJ. Characterization of *eds1*, a
502 mutation in Arabidopsis suppressing resistance to *Peronospora parasitica* specified by
503 several different *RPP* genes. Plant Cell. 1996;8: 2033–2046. doi:10.1105/tpc.8.11.2033

504 **37.** Aarts N, Metz M, Holub E, Staskawicz BJ, Daniels MJ, Parker JE. Different requirements
505 for *EDS1* and NDR1 by disease resistance genes define at least two *R* gene-mediated
506 signaling pathways in Arabidopsis. Proc Natl Acad Sci U S A. 1998;95: 10306–10311.
507 doi:10.1073/pnas.95.17.10306
508 **38.** Falk A, Feys BJ, Frost LN, Jones JD, Daniels MJ, Parker JE. *EDS1*, an essential component
509 of *R* gene-mediated disease resistance in Arabidopsis has homology to eukaryotic lipases.
510 Proc Natl Acad Sci U S A. 1999;96: 3292–3297. doi:10.1073/pnas.96.6.3292
511 **39.** Feys BJ, Moisan LJ, Newman MA, Parker JE. Direct interaction between the Arabidopsis
512 disease resistance signaling proteins, EDS1 and PAD4. EMBO J. 2001;20: 5400–5411.
513 doi:10.1093/emboj/20.19.5400
514 **40.** Li Y, Yang S, Yang H, Hua J. The TIR-NB-LRR gene *SNC1* is regulated at the transcript
515 level by multiple factors. Mol Plant-Microbe Interact MPMI. 2007;20: 1449–1456.
516 doi:10.1094/MPMI-20-11-1449
517 **41.** Zhang N, Wang Z, Bao Z, Yang L, Wu D, Shu X, et al. MOS1 functions closely with TCP
518 transcription factors to modulate immunity and cell cycle in Arabidopsis. Plant J Cell Mol
519 Biol. 2018;93: 66–78. doi:10.1111/tpj.13757
520 **42.** Alonso JM, Stepanova AN, Leisse TJ, Kim CJ, Chen H, Shinn P, et al. Genome-wide
521 insertional mutagenesis of *Arabidopsis thaliana*. Science. 2003;301: 653–657.
522 doi:10.1126/science.1086391
523 **43.** Sessions A, Burke E, Presting G, Aux G, McElver J, Patton D, et al. A high-throughput
524 Arabidopsis reverse genetics system. Plant Cell. 2002;14: 2985–2994.
525 doi:10.1105/tpc.004630

526 **44.** Nakagawa T, Kurose T, Hino T, Tanaka K, Kawamukai M, Niwa Y, et al. Development of
527 series of gateway binary vectors, pGWBs, for realizing efficient construction of fusion
528 genes for plant transformation. J Biosci Bioeng. 2007;104: 34–41. doi:10.1263/jbb.104.34
529 **45.** Ruijter JM, Ramakers C, Hoogaars WMH, Karlen Y, Bakker O, van den Hoff MJB, et al.
530 Amplification efficiency: linking baseline and bias in the analysis of quantitative PCR data.
531 Nucleic Acids Res. 2009;37: e45. doi:10.1093/nar/gkp045
532 **46.** Livak KJ, Schmittgen TD. Analysis of relative gene expression data using real-time
533 quantitative PCR and the 2(-Delta Delta C(T)) Method. Methods San Diego Calif. 2001;25:
534 402–408. doi:10.1006/meth.2001.1262
535
536

Figure Legends

Fig 1. Loss of function of *TPR2* increases stunting in *srfr1*.

(A) Morphological phenotype of *srfr1-4* and *srfr1-4 tpl/tpr* double mutants at four weeks post sowing. (B) Shoot weight from plants grown under short day conditions at 21ºC for four weeks. Dots represent individual data points taken over two separate experiments. Whiskers on boxplots are drawn to the farthest data point within 1.5 * IQR of first and third quartiles. Letters denote significant differences as determined by Student's t-test (P<0.01) using the Bonferroni-Holm method to correct for multiple comparisons.

Fig 2. Multiple alleles of *TPR2* increase stunting in *srfr1*.

(A) Morphological phenotypes of *tpr2-1*, *tpr2-2*, *srfr1-4*, *srfr1-4 tpr2-1*, and *srfr1-4 tpr2-2* at four weeks post sowing. (B) Shoot weight from plants grown under short day conditions at 21ºC for four weeks. Dots represent individual data points. Whiskers on boxplots are drawn to the farthest data point within 1.5 * IQR of first and third quartiles. Letters denote significant differences as determined by Student's t-test (P<0.05) using the Bonferroni-Holm method to correct for multiple comparisons.

Fig 3. Simultaneous loss of *TPR2* and *TPR3* increases stunting and expression of *PR2* and *SNC1* in *srfr1*.

(A) Morphological phenotype of *srfr1-4*, *srfr1-4 tpr2-2*, and *srfr1-4 tpr2-2 tpr3-1* at 20 days after sowing. Plants were grown under short day conditions at 21ºC. (B) Shoot weight from plants grown under short day conditions at 21ºC for four weeks. Dots represent individual data points

taken over two separate experiments. Whiskers on boxplots are drawn to the farthest data point within 1.5 * IQR of first and third quartiles. Letters denote significant differences as determined by Student's t-test (P<0.001) using the Bonferroni-Holm method to correct for multiple comparisons. (C&D) Expression as measured by quantitative RT-PCR of *PR2* and *SNC1* in single, double, and triple mutants. Dots represent individual data points taken over two separate experiments. Genes of interest were normalized against *SAND* (At2g28390). Whiskers on boxplots are drawn to the farthest data point within 1.5 * IQR of first and third quartiles. Letters denote significant differences as determined by Student's t-test (P<0.05) using the Bonferroni-Holm method to correct for multiple comparisons.

Fig 4. *SNC1* expression is increased in *tpr2 tpr3*

(A) Morphological phenotype of *tpr2-2 tpr3-1*. Plants were grown for four weeks under short day conditions at 21ºC. (B&C) Expression as measured by quantitative RT-PCR of *PR2* and *SNC1*. Dots represent individual data points taken over two separate experiments. Genes of interest were normalized against *SAND* (At2g28390). Whiskers on boxplots are drawn to the farthest data point within 1.5 * IQR of first and third quartiles. Asterisks denote significant differences as determined by Student's t-test (P<0.005) using the Bonferroni-Holm method to correct for multiple comparisons.

Fig 5. Overexpression of TPR2 reduces stunting and *SNC1* expression in *srfr1 tpr2*

(A) Morphological phenotype of *TPR2-myc srfr1-4 tpr2-2* compared to *srfr1-4* and *srfr1-4 tpr2-2*. Plants were grown under short day conditions at 21ºC for four weeks. (B&C) Expression as measured by quantitative RT-PCR of *SNC1* and *RPP4*. Dots represent individual data points

583 taken over two separate experiments. Genes of interest were normalized against *SAND*
584 (At2g28390). Whiskers on boxplots are drawn to the farthest data point within 1.5 * IQR of first
585 and third quartiles. Letters denote significant differences as determined by Student's t-test
586 (P<0.05) using the Bonferroni-Holm method to correct for multiple comparisons.
587
588 **Fig 6. *tpr2 tpr3* mutants have lower expression of *RPP4* in *snc1* knockouts**
589 (A) Morphological phenotype of plants harboring the *snc1-11* mutation crossed into *srfr1* and
590 *tpr2 tpr3* mutants. Plants were grown under short day conditions at 21ºC for four weeks. (B&C)
591 Expression as measured by quantitative RT-PCR of *RPP4* and *PR2.* Dots represent individual
592 data points taken over two separate experiments. Genes of interest were normalized against
593 *SAND* (At2g28390). Whiskers on boxplots are drawn to the farthest data point within 1.5 * IQR
594 of first and third quartiles. Letters denote significant differences as determined by Student's t-test
595 (P<0.05) using the Bonferroni-Holm method to correct for multiple comparisons.
596
597 **Fig 7. Mutations in *TPR2* increase stunting and *SNC1* expression in *snc1-1* mutants**
598 (A) Morphological phenotypes of *snc1-1* and *snc1-1 tpr2-2*. Plants were grown under short day
599 conditions at 21ºC for four weeks. (B&C) Expression as measured by quantitative RT-PCR of
600 *SNC1* and *PR2.* Dots represent individual data points taken over two separate experiments.
601 Genes of interest were normalized against *SAND* (At2g28390). Whiskers on boxplots are drawn
602 to the farthest data point within 1.5 * IQR of first and third quartiles. Letters denote significant
603 differences as determined by Student's t-test (P<0.01) using the Bonferroni-Holm method to
604 correct for multiple comparisons.
605

606 **Fig 8. SRFR1 acts upstream of SNC1 transcription**

607 (A) Morphological phenotypes of single, double, and triple mutants of *eds1-2*, *srfr1-4*, and *tpr2-*
608 *2*. Plants were grown under short day conditions at 21ºC for four weeks. (B) Expression as
609 measured by quantitative RT-PCR of *SNC1.* Dots represent individual data points taken over two
610 separate experiments. Genes of interest were normalized against *SAND* (At2g28390). Whiskers
611 on boxplots are drawn to the farthest data point within 1.5 * IQR of first and third quartiles.
612 Letters denote significant differences as determined by Student's t-test (P<0.01) using the
613 Bonferroni-Holm method to correct for multiple comparisons. (C) *In vitro* interaction of TPR2
614 and the TIR domain of SNC1 in *E. coli.* Proteins were pulled down and subjected to immunoblot
615 analysis with either GST or T7 antibodies. This experiment was repeated once with similar
616 results.

617

618 **Fig 9. Model for TPR2/TPR3 and SRFR1 functions in SNC1-mediated autoimmunity**

619 (Left) In Col-0, low levels of *SNC1* help to avoid fitness penalties. This may be accomplished
620 both through direct inhibition by SRFR1 and through competitive inhibition by TPR2 (additively
621 with TPR3) of the demonstrated TPR1-SNC1 interaction that affects negative regulators of
622 immunity such as *DND1/DND2* and indirectly subsequent *SNC1* expression. Here, the combined
623 effects of SRFR1 and TPR2 hold SNC1 expression in check. (Right) In the *srfr1-4 tpr2-2 tpr3-*
624 *1* triple mutant, these molecular check points are released, allowing SNC1 expression to trigger
625 an autoimmune response that results in excessive stunting.

626

627

628

S1 Fig. PR2 expression in *srfr1-4* is affected by *tpl* and *tpr2*

Western blot of total protein extracted from *srfr1-4, srfr1-4 tpl-8*, *srfr1-4 tpr1-2*, *srfr1-4 tpr2-2*, *srfr1-4 tpr3-1*, and *srfr1-4 tpr4-1*. The large subunit of rubisco is shown as a loading control.

S2 Fig. Phylogenetic tree of the Arabidopsis thaliana TOPLESS family

Phylogram showing evolutionary relationships amongst *TOPLESS* family members. The WD40 protein *LEUNIG* (*LUG*) is included as the outgroup. Tree was generated from full length cDNA sequences using www.phylogeny.fr.

S1 Table. PCR primers used for genotyping mutant lines

S2 Table. Primers used for qPCR

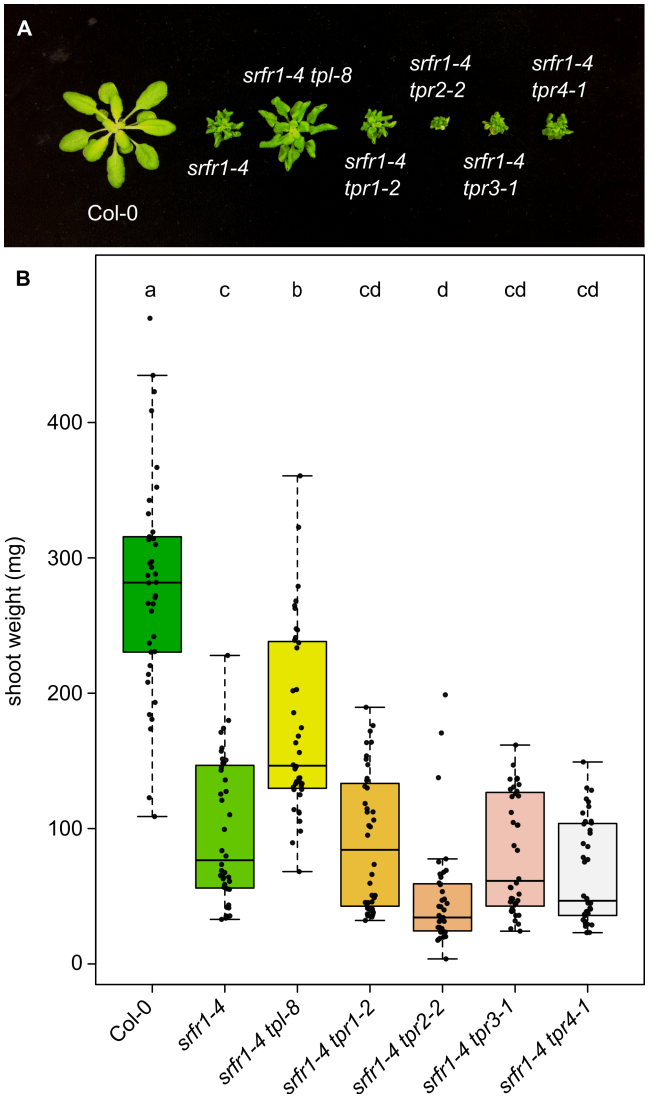

Fig 1. Loss of function of *TPR2* increases stunting in *srfr1*.
(A) Morphological phenotype of *srfr1-4* and *srfr1-4 tpl/tpr* double mutants at four weeks post sowing. (B) Shoot weight from plants grown under short day conditions at 21ºC for four weeks. Dots represent individual data points taken over two separate experiments. Whiskers on boxplots are drawn to the farthest data point within 1.5 * IQR of first and third quartiles. Letters denote significant differences as determined by Student's t-test (P<0.01) using the Bonferroni-Holm method to correct for multiple comparisons.

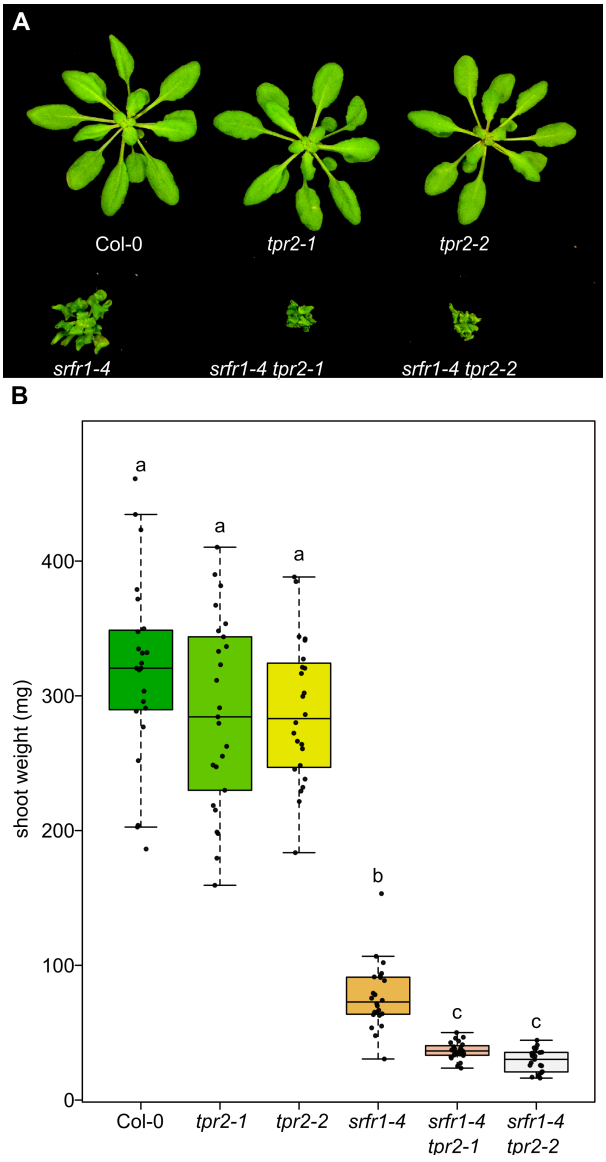

Fig 2. Multiple alleles of *TPR2* increase stunting in *srfr1*.
(A) Morphological phenotypes of *tpr2-1*, *tpr2-2*, *srfr1-4*, *srfr1-4 tpr2-1*, and *srfr1-4 tpr2-2* at four weeks post sowing. (B) Shoot weight from plants grown under short day conditions at 21ºC for four weeks. Dots represent individual data points. Whiskers on boxplots are drawn to the farthest data point within 1.5 * IQR of first and third quartiles. Letters denote significant differences as determined by Student's t-test (P<0.05) using the Bonferroni-Holm method to correct for multiple comparisons.

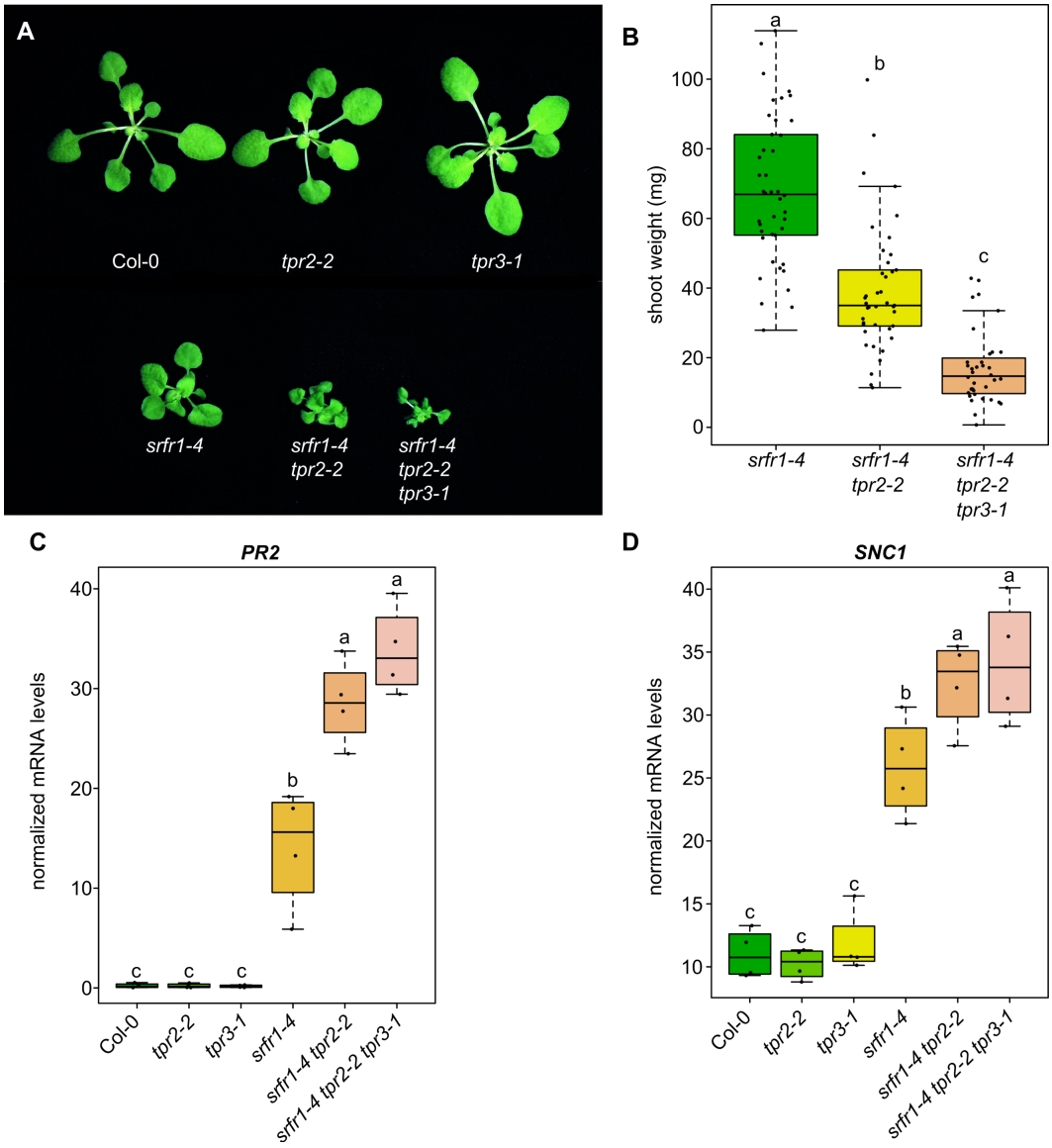

Fig 3. Simultaneous loss of *TPR2* and *TPR3* increases stunting and expression of *PR2* and *SNC1* in *srfr1*.

(A) Morphological phenotype of *srfr1-4*, *srfr1-4 tpr2-2*, and *srfr1-4 tpr2-2 tpr3-1* at 20 days after sowing. Plants were grown under short day conditions at 21ºC. (B) Shoot weight from plants grown under short day conditions at 21ºC for four weeks. Dots represent individual data points taken over two separate experiments. Whiskers on boxplots are drawn to the farthest data point within 1.5 * IQR of first and third quartiles. Letters denote significant differences as determined by Student's t-test (P<0.001) using the Bonferroni-Holm method to correct for multiple comparisons. (C&D) Expression as measured by quantitative RT-PCR of *PR2* and *SNC1* in single, double, and triple mutants. Dots represent individual data points taken over two separate experiments. Genes of interest were normalized against *SAND* (At2g28390). Whiskers on boxplots are drawn to the farthest data point within 1.5 * IQR of first and third quartiles. Letters denote significant differences as determined by Student's t-test (P<0.05) using the Bonferroni-Holm method to correct for multiple comparisons.

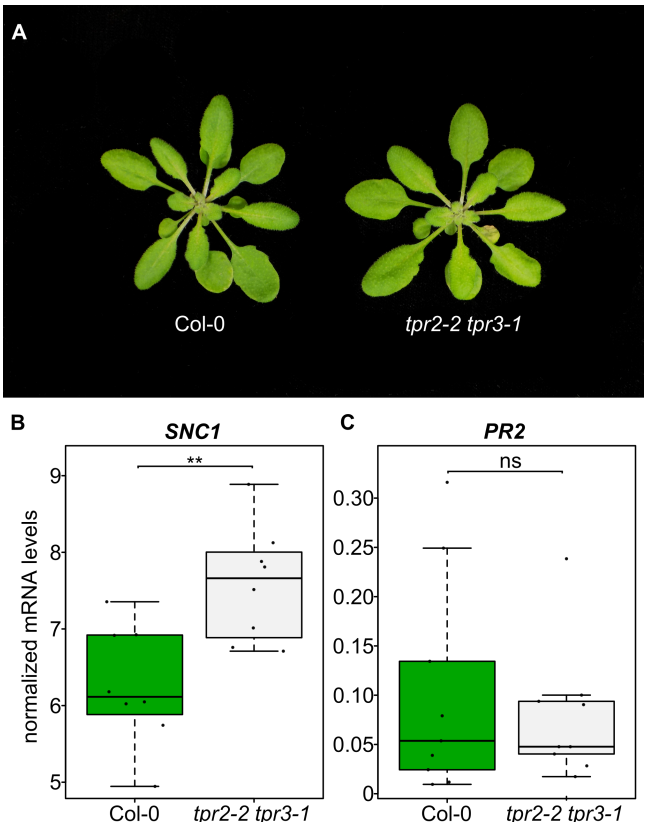

Fig 4. *SNC1* expression is increased in *tpr2 tpr3*

(A) Morphological phenotype of *tpr2-2 tpr3-1*. Plants were grown for four weeks under short day conditions at 21ºC. (B&C) Expression as measured by quantitative RT-PCR of *PR2* and *SNC1*. Dots represent individual data points taken over two separate experiments. Genes of interest were normalized against *SAND* (At2g28390). Whiskers on boxplots are drawn to the farthest data point within 1.5 * IQR of first and third quartiles. Asterisks denote significant differences as determined by Student's t-test (P<0.005) using the Bonferroni-Holm method to correct for multiple comparisons.

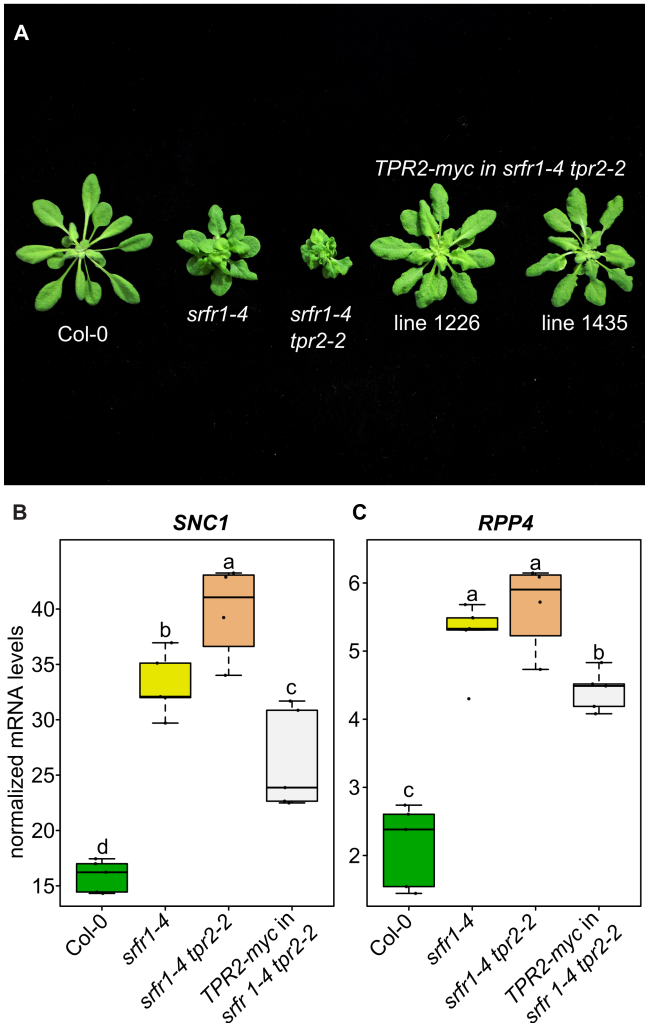

Fig 5. Overexpression of TPR2 reduces stunting and *SNC1* expression in *srfr1 tpr2*
(A) Morphological phenotype of *TPR2-myc srfr1-4 tpr2-2* compared to *srfr1-4* and *srfr1-4 tpr2-2*. Plants were grown under short day conditions at 21ºC for four weeks. (B&C) Expression as measured by quantitative RT-PCR of *SNC1* and *RPP4.* Dots represent individual data points taken over two separate experiments. Genes of interest were normalized against *SAND* (At2g28390). Whiskers on boxplots are drawn to the farthest data point within 1.5 * IQR of first and third quartiles. Letters denote significant differences as determined by Student's t-test (P<0.05) using the Bonferroni-Holm method to correct for multiple comparisons.

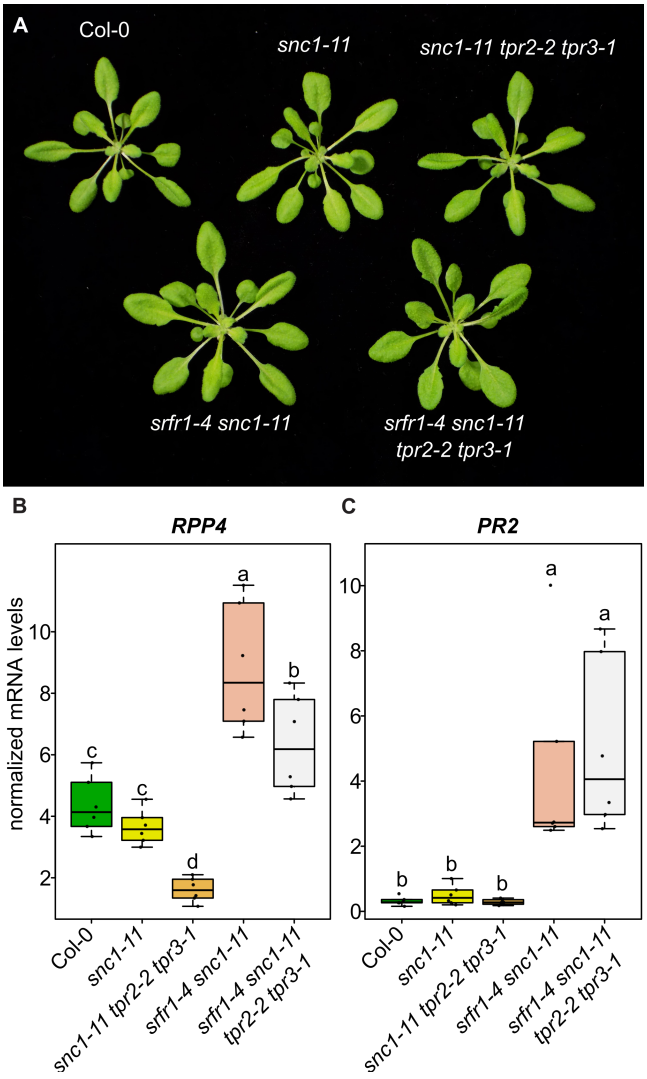

Fig 6. *tpr2 tpr3* mutants have lower expression of *RPP4* in *snc1* knockouts
(A) Morphological phenotype of plants harboring the *snc1-11* mutation crossed into *srfr1* and *tpr2 tpr3* mutants. Plants were grown under short day conditions at 21ºC for four weeks. (B&C) Expression as measured by quantitative RT-PCR of *RPP4* and *PR2*. Dots represent individual data points taken over two separate experiments. Genes of interest were normalized against *SAND* (At2g28390). Whiskers on boxplots are drawn to the farthest data point within 1.5 * IQR of first and third quartiles. Letters denote significant differences as determined by Student's t-test (P<0.05) using the Bonferroni-Holm method to correct for multiple comparisons.

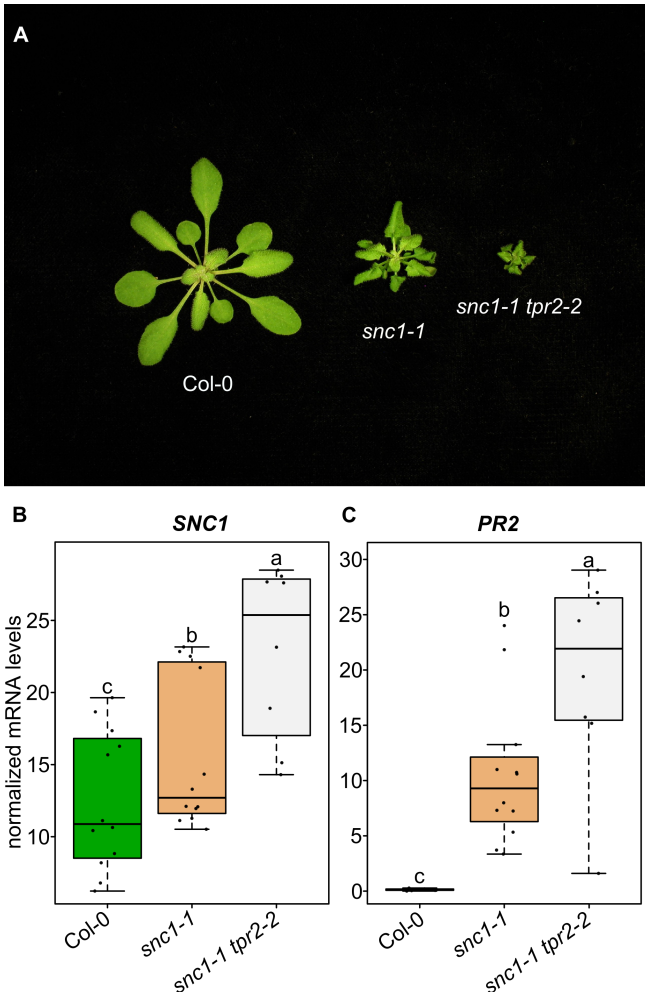

Fig 7. Mutations in *TPR2* increase stunting and *SNC1* expression in *snc1-1* mutants
(A) Morphological phenotypes of *snc1-1* and *snc1-1 tpr2-2*. Plants were grown under short day conditions at 21ºC for four weeks. (B&C) Expression as measured by quantitative RT-PCR of *SNC1* and *PR2.* Dots represent individual data points taken over two separate experiments. Genes of interest were normalized against *SAND* (At2g28390). Whiskers on boxplots are drawn to the farthest data point within 1.5 * IQR of first and third quartiles. Letters denote significant differences as determined by Student's t-test (P<0.01) using the Bonferroni-Holm method to correct for multiple comparisons.

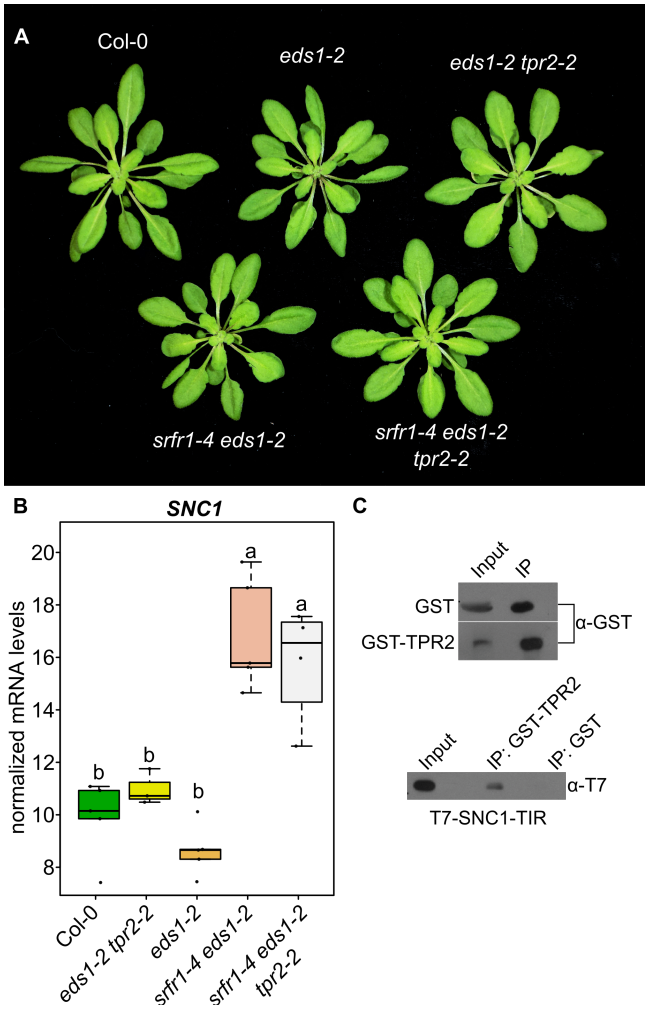

Fig 8. SRFR1 acts upstream of SNC1 transcription

(A) Morphological phenotypes of single, double, and triple mutants of *eds1-2*, *srfr1-4*, and *tpr2-2*. Plants were grown under short day conditions at 21ºC for four weeks. (B) Expression as measured by quantitative RT-PCR of *SNC1*. Dots represent individual data points taken over two separate experiments. Genes of interest were normalized against *SAND* (At2g28390). Whiskers on boxplots are drawn to the farthest data point within 1.5 * IQR of first and third quartiles. Letters denote significant differences as determined by Student's t-test (P<0.01) using the Bonferroni-Holm method to correct for multiple comparisons. (C) *In vitro* interaction of TPR2 and the TIR domain of SNC1 in *E. coli.* Proteins were pulled down and subjected to immunoblot analysis with either GST or T7 antibodies. This experiment was repeated once with similar results.

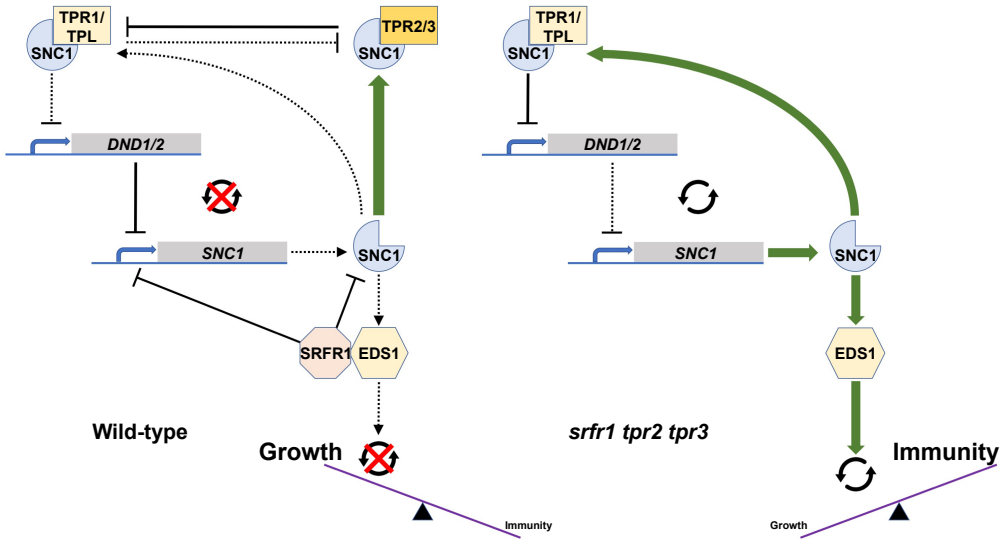

Fig 9. Model for TPR2/TPR3 and SRFR1 functions in SNC1-mediated autoimmunity
(Left) In Col-0, low levels of *SNC1* help to avoid fitness penalties. This may be accomplished both through direct inhibition by SRFR1 and through competitive inhibition by TPR2 (additively with TPR3) of the demonstrated TPR1-SNC1 interaction that affects negative regulators of immunity such as *DND1/DND2* and indirectly subsequent *SNC1* expression. Here, the combined effects of SRFR1 and TPR2 hold SNC1 expression in check. (Right) In the *srfr1-4 tpr2-2 tpr3-1* triple mutant, these molecular check points are released, allowing SNC1 expression to trigger an autoimmune response that results in excessive stunting.

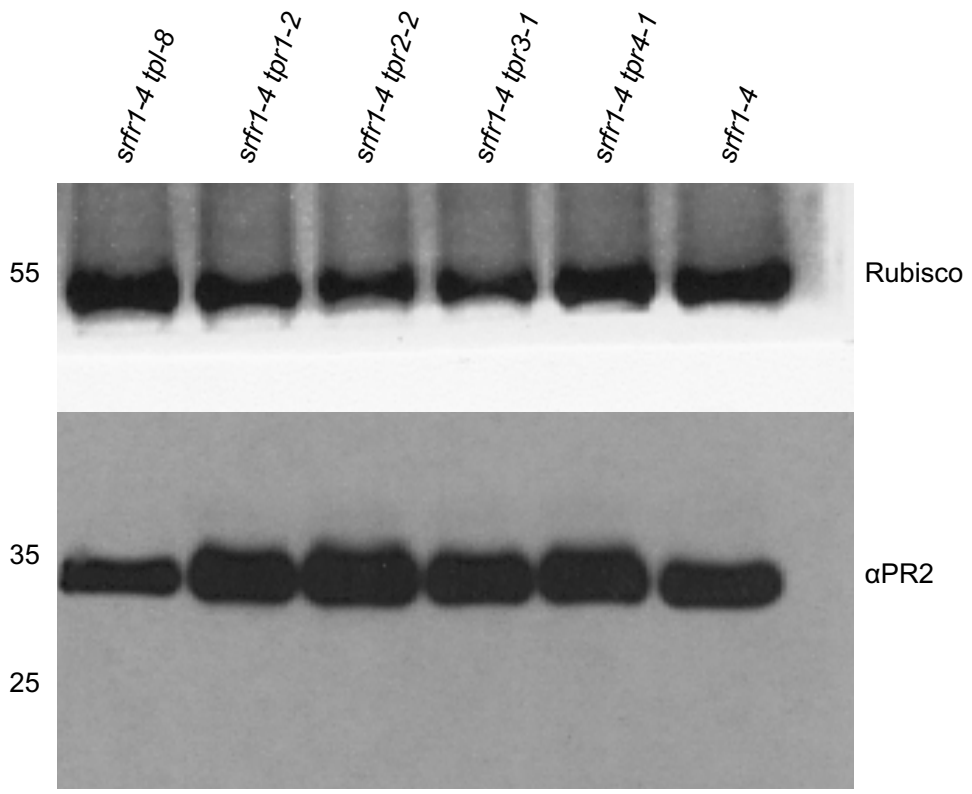

S1 Fig. PR2 expression in *srfr1-4* is affected by *tpl* and *tpr2*
Western blot of total protein extracted from *srfr1-4, srfr1-4 tpl-8*, *srfr1-4 tpr1-2*, *srfr1-4 tpr2-2*, *srfr1-4 tpr3-1*, and *srfr1-4 tpr4-1*. The large subunit of rubisco is shown as a loading control.

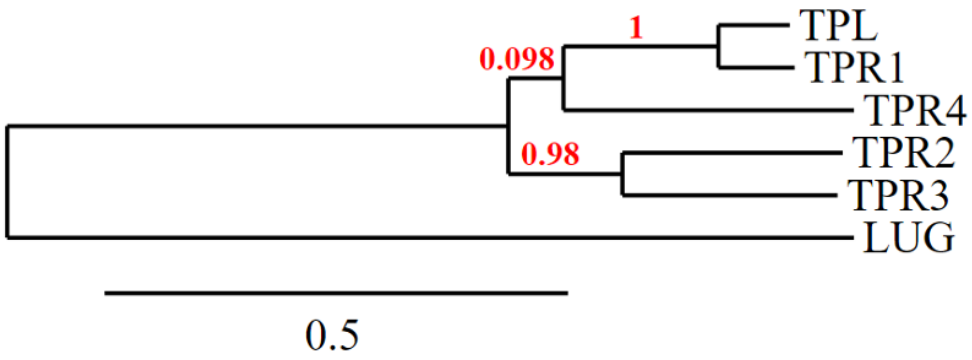

S2 Fig. Phylogenetic tree of the Arabidopsis thaliana TOPLESS family
Phylogram showing evolutionary relationships amongst *TOPLESS* family members. The WD40 protein *LEUNIG* (*LUG*) is included as the outgroup. Tree was generated from full length cDNA sequences using www.phylogeny.fr.

S1 Table. PCR primers used for genotyping mutant lines

Name	sequence	Use
LBa1	TGGTTCACGTAGTGGGCCATCG	SALK line border primer
TPL8 LP	TTGGTTCTCGCGAAAGATTAG	tpl-8
TPL8 RP	AGGAGAGAGCCTTCCTTGTTG	tpl-8
TPR1-2 LP	AAGGCCTCGAGATACTTCTGC	tpr1-2
TPR1-2 RP	ACTCCGTTATCCGTCACCTTC	tpr1-2
TPR2-2 LP	TCAGCATCAAAGACTGCAATG	tpr2-2
TPR2-2 RP	TGGGAAGGTGATTCGTTGTAC	tpr2-2
TPR2-1 LP	TCCTTGTTGAATCTCAATCGG	tpr2-1
TPR2-1 RP	ACGTCAACACCTCGAGGTATG	tpr2-1
TPR3-1LP	GTTCTCTTGCAGCCTCAATTG	tpr3-1
TPR3-1RP	TTCCCACAATGTGATTTCTCC	tpr3-1
TPR4-1 GTF	ATGTCGTCACTCAGCAGAGAACTC	tpr4-1
TPR4-1 GTR	GCAAAGCTGATGTTGCCAGTTCAA	tpr4-1
SNC1-11 LP	TCGGCATAACATCGTAAGAGC	snc1-11
SNC1-11 RP	CAAGCTTTCGTGGAGAAGATG	snc1-11
SNC1 FOR GT	GGCATGCGTAATCTGCAATATCTAG	snc1-1
SNC1 LESLEY REV	GAGGTACTCGAGAGATTCCAAGTTG	snc1-1
SNC1-1 GT FOR	GGCATGCGTAATCTGCAATATCTAa	snc1-1
37460-18	TCTCCACTGTACTAATTTCCCT	srfr1-4
37460-R	ACTAATTCCGCAACGTGCCT	srfr1-4
EDS1 F2	CCCTTTCTAGTTTCCTTGAGCTAAG	eds1-2
EDS1 R3	TCAGGTATCTGTTATTTCATCCATC	eds1-2

S2 Table. Primers used for qPCR

Primer name	sequence
SAND CDNA FOR 1	CACTTGCAGACAAGGCGATG
SAND CDNA REV 1	CCTTTGGCACACCTGATTGC
TPR2 CDNA FOR4	ATTATTGCAATCGGGATGGA
TPR2 CDNA RP5	CTTGGGGCACCCACTTATGA
QRT SNC1 FOR1	GCGGTGTACGACTCATGTATGTC
QRT SNC1 REV1	GATGTCATCCGCATCCGCTT
PR2 QRT FOR1	TTCAACCACACAGCTGGACA
PR2 QRT REV1	GGCAAGGTATCGCCTAGCAT
RPP4 QRT FOR1	GGAAGGCATCCAGTCGCTT
RPP4 QRT REV1	CACCAAACTTTTGCACCCGT